Searching for New Mathematical Growth Model Approaches for *Listeria monocytogenes*

A. VALERO, C. HERVÁS, R.M. GARCÍA-GIMENO, AND G. ZURERA

ABSTRACT: Different secondary modeling approaches for the estimation of *Listeria monocytogenes* growth rate as a function of temperature (4 to 30 °C), citric acid (0% to 0.4% w/v), and ascorbic acid (0% to 0.4% w/v) are presented. Response surface (RS) and square-root (SR) models are proposed together with different artificial neural networks (ANN) based on product functions units (PU), sigmoidal functions units (SU), and a novel approach based on the use of hybrid functions units (PSU), which results from a combination of PU and SU. In this study, a significantly better goodness-of-fit was obtained in the case of the ANN models presented, reflected by the lower SEP values obtained (< 24.23 for both training and generalization datasets). Among these models, the SU model provided the best generalization capacity, displaying lower RMSE and SEP values, with fewer parameters compared to the PU and PSU models. The bias factor (B_f) and accuracy factor (A_f) of the mathematical validation dataset were above 1 in all cases, providing fail-safe predictions. The balance between generalization properties and the ease of use is the main consideration when applying secondary modeling approaches to achieve accurate predictions about the behavior of microorganisms.

Keywords: artificial neural networks, growth models, predictive microbiology, *Listeria monocytogenes*

Introduction

Predictive microbiology is a specific application of the field of mathematical modeling for describing the behavior of pathogen and spoilage microorganisms under a given set of environmental conditions. Growth predictive models have been widely accepted as informative tools that provide quick and cost-effective assessments of microbial growth for product development, risk assessment, and educational purposes (Ross 1999). Although there are several classifications of predictive models, the one proposed by Whiting and Buchanan (1993) (primary, secondary, and tertiary models) is currently the most commonly used classification.

This paper focuses on secondary type models. In predictive microbiology, the development and application of secondary models for growth rate and lag time have been extensively reviewed (McClure and others 1997; Devlieghere and others 2000, 2001; Zurera-Cosano and others 2004). Square-root models describe the effect of suboptimal temperature on growth rate (Ratkowsky and others 1982). When this initial model is fitted to experimental growth rates, the data are square-transformed to stabilize their variance. This empirical relationship was transformed into a multiplicative model to consider the effect of additional environmental parameters such as CO_2, sodium lactate, or water activity (Dalgaard and others 1997; Devlieghere and others 2000, 2001). One of the major advantages of these models is the fact that they are simple, easy to interpret, and use few parameters. Furthermore, the biological significance of microorganisms behavior can be obtained from the restricted parameters.

Polynomial models were extensively used in the 1990s, being the most common secondary models. They do provide certain advantages; for example, it is easy to fit heterogeneous groups of experimental data using multiple linear regression techniques. Such models commonly use response surface analysis and have been used to predict growth as a function of factors such as pH, NaCl, temperature, and other preservatives (Buchanan and Phillips 1993 Wijtzes and others 1993; McClure and others 1997). However, these models often produce an excessive number of parameters and lack biological interpretability.

Artificial neural networks (ANN) have been proposed as useful tools for modeling complex nonlinear systems (Hajmeer and others 1997). Their applications in predictive microbiology field are used for modeling growth curves as a function of extrinsic and intrinsic parameters (Geeraerd and others 1998; Jeyamkondan and others 2001; García-Gimeno and others 2003, 2005). Their major advantages are the approximation of underlying relationships of any complexity between the independent variables and their flexibility to fit bacterial growth data, especially in dynamic conditions (Cheroutre-Vialette and Lebert 2002). Traditional models refer to Multi-Layer Perceptron type (MLP) models: this group includes sigmoidal-base unit functions (SU) and also multiplicative networks including product-base unit functions (PU). In addition to these groups of models, where hidden layer nodes have the same activation/transfer functions, hybrid models can include different functions. A few studies have focused on this area, such as Cohen and Intrator (2002, 2005), who compared sigmoidal-base, product-base, and radial-base unit functions. As described by Geeraerd and others (2004), the generalization properties of growth models (in other words, the performance of the model when confronted with new data) are essential to assess their predictive capacity. Generally speaking, a lower goodness-of-fit is reasonably acceptable in certain cases if the generalization capacity is improved. Although almost all models used have drawbacks in their utilization, it is important to select an appropriate model for a specific dataset.

Mild-preservation technologies are increasing due to the major demand of nature and fresh products (Jacxsens and others 2003). The effect of citric acid (CA) has been proven to be both protective

MS 20060269 Submitted 5/11/2006, Accepted 10/6/2006. *Authors Valero, García-Gimeno, and Zurera are with Dept. of Food Science and Technology, Univ. of Cordoba, Campus Univ. de Rabanales, 14014 Córdoba, Spain. Authors Hervás is with Dept. of Computing, Univ. of Cordoba, Campus Univ. de Rabanales, 14014 Córdoba, Spain. Direct inquiries to author Valero (E-mail: bt2vadia@uco.es).*

doi: 10.1111/j.1750-3841.2006.00208.x

and bactericidal against *Listeria monocytogenes* (Buchanan and Golden 1994). Ascorbic acid (AA) is added to a variety of foods to improve their quality or to enhance their nutritional value (Mackey and Seymour 1989) having either bacteriostatic or a bactericidal activity (Eddy and Ingram1953). Moreover, the combination of low temperature, low pH, and high concentration of organic acids can inhibit the growth of *L. monocytogenes* in minimally processed foods (Le Marc and others 2002).

The main purpose of this study is to present and compare the applicability of different secondary model approaches on a dataset of *L. monocytogenes* growth rate as a function of storage temperature, CA, and AA: (i) square-root model (SR), (ii) response surface model (RS), and (iii) the use of ANN models associated with sigmoidal, product base functions, and hybrid models.

Materials and Methods

Strain and preculture conditions

A slant culture containing *L. monocytogenes* (strain NCTC 11994) was incubated for 24 h at 30 °C in 10 mL of pure tryptone soya broth (TSB, pH 7.2). Then, 1 mL of the culture was incubeted in a test tube of 9 mL of TSB (24 h, 30 °C each). A 3rd subculture was obtained in the same way, incubating 1 mL of the inoculum in a flask of 100 mL of TSB until the early stationary phase was reached.

Sample preparation and growth evaluation

Modified media were achieved by adding all possible combinations of concentrations of CA L (−) 1-hydrate and L (+) AA (0% to 0.4% w/v) to 100 mL of TSB. Following sterilization of the media, the final pH was checked (Table 1).

Growth was assessed by measuring absorbance in Bioscreen C at 600 nm. Prior to inoculation, microtiter plates with 10 × 10 wells were filled with 160 μL of modified media. Each condition was replicated 5 times and 2 blank samples with 200 μL each were run. Then, the inoculum size was adjusted by a calibration curve (30 °C, pH 7.2) until a concentration of approximately 10^6 CFU/mL was obtained. Finally, the wells were inoculated with 40 μL of inoculum. Log-absorbance data were obtained as a function of time for each condition tested.

Table 1—Combinations of organic acids performed for model and validation datasets. Final pHs for each condition are also shown.

	Model dataset		Validation dataset		
CA (%)	AA (%)	pH	CA (%)	AA (%)	pH
0	0	7.26	0	0.05	7.08
0	0.1	6.92	0.05	0	6.31
0	0.2	6.79	0.05	0.05	6.27
0	0.3	6.62	0.05	0.15	6.07
0	0.4	6.37	0.05	0.25	5.8
0.1	0	6.34	0.05	0.35	5.5
0.1	0.1	5.92	0	0.15	6.22
0.1	0.2	5.64	0.15	0	6.09
0.1	0.3	5.46	0.15	0.05	6.01
0.1	0.4	5.38	0.15	0.15	5.84
0.2	0	5.67	0.15	0.25	5.63
0.2	0.1	5.47	0.15	0.35	5.4
0.2	0.2	5.38	0	0.25	5.98
0.2	0.3	5.16	0.25	0	5.85
0.2	0.4	4.95	0.25	0.05	5.79
0.3	0	5.37	0.25	0.15	5.64
0.3	0.1	5.33	0.25	0.25	5.46
0.3	0.2	5.13	0.25	0.35	5.32
0.3	0.3	4.76	0	0.35	5.74
0.3	0.4	4.5	0.35	0	5.51
0.4	0	5	0.35	0.05	5.4
0.4	0.1	4.86	0.35	0.15	5.19
0.4	0.2	4.71	0.35	0.25	4.97
0.4	0.3	4.6	0.35	0.35	4.84
0.4	0.4	4.41			

Experimental data

The experimental design was based on an enlarged dataset from the study of Carrasco and others (2006). All possible combinations of factors were performed within the following intervals for the conditions studied: storage temperature (4, 7, 10, 15, 20, 25, 30 °C); CA concentration (0%; 0.1%; 0.2%; 0.3%; 0.4% w/v) and AA concentration (0%; 0.1%; 0.2%; 0.3%; 0.4% w/v).

To validate the performance of the model (that is, to test the generalization capabilities), additional conditions were tested within the experimental range of the datasets mentioned above. These additional conditions are at the same temperature values, but other CA and AA concentrations (0%, 0.05%, 0.15%, 0.25%, and 0.35% w/v) (Table 1).

Relation between absorbance and cell count

Calibration curves performed at different combinations of temperature (4 to 30 °C) and pH (4.5 to 7.2) were used to transform absorbance data to cell counts (Table 2). Modified TSB was prepared by adding CA L (−) 1-hydrate and L (+) AA to 100 mL of culture medium as necessary. The pH of TSB was modified in order to cover the entire pH range reached in the experiment. After autoclaving, the final pH was checked. To perform calibration curves, *L. monocytogenes* cells were grown for 24 h at 30 °C in TSB from a slant culture. Later, 1 mL was transferred into 10 mL of TSB and incubated at 30 °C for 24 h. A 3rd subculture was incubated in a flask of 100 mL of pH-modified TSB medium, at different temperatures until the early stationary phase was reached.

Table 2—Criteria followed for applying the calibration curves to growth model conditions at different levels of T and pH

Calibration curves		Growth model conditions	
T (°C)	pH	T (°C)	pH range
30	7.2	30	6.5–7.2
		25	6.5–7.2
		20	6.5–7.2
30	6	30	5.75–6.5
		25	5.75–6.5
		20	5.75–6.5
30	5.5	30	5.25–5.75
		25	5.25–5.75
		20	5.25–5.75
30	5	30	4.75–5.25
		25	4.75–5.25
		20	4.75–5.25
30	4.5	30	<4.75
		25	<4.75
		20	<4.75
15	7.2	15	6.5–7.2
15	6	15	5.75–6.5
15	5.5	15	5.25–5.75
15	5	15	4.75–5.25
15	4.5	15	<4.75
10	7.2	10	6.5–7.2
10	6	10	5.75–6.5
10	5.5	10	5.25–5.75
10	5	10	4.75–5.25
7	7.2	7	6.5–7.2
7	6	7	5.75–6.5
7	5.5	7	5.25–5.75
4	7.2	4	6.5–7.2
4	6	4	5.75–6.5

Calibration curves were performed in accordance with the protocol defined by Francois and others (2005) for each combination tested in order to study the relationship between absorbance and cell count in a microtiter plate. From the initial inoculum, a half dilution series was made in TSB in a microtiter plate. In the 1st column, 200 μL inoculum was added to all the wells using a multipipet, where initially all other wells were filled with 200 μL of broth. In each well of the 2nd column, 200 μL inoculum was added to 200 μL broth. From each of those wells, 200 μL was taken to prepare the next dilution. This procedure resulted in 10 dilution steps, each in 10 replicates.

The inoculum size was controlled by making dilution series in TSB and plating on tryptone soya agar, then incubating at 30 °C for 24 h. Microtiter plates were placed in Bioscreen C and absorbance measurements were taken. Measurements were corrected by a blank containing only TSB. A logarithmic transformation was performed for both absorbance values and cell count data to standardize the variance and the distance between the data points. These transformed data were used to fit linear regression curves in Microsoft Excel™. The main statistical parameters and the goodness-of-fit (R^2 adjusted and standard deviation) for each regression curve are shown in Table 3.

Data fitting: primary model

The DMFit 1.0 curve fitting program was used to fit cell count data as a function of time by applying the Baranyi and Roberts function (1994). Previously, cell count data were log transformed in order to standardize the variance. Using this primary model, the growth rate (μ) was estimated.

Secondary modeling approaches

Square-root model (SR). The estimates obtained for μ (h^{-1}) were primarily fitted using the Ratkowsky model (Ratkowsky and others 1982) to consider the effect of temperature on the growth rate of *L. monocytogenes* as described in Eq. 1. Based on the study of Devlieghere and others (2000), this model was extended to the amount of CA and AA in order to observe the effect of these factors on μ. The model has the following form:

$$\sqrt{\mu} = a + b(X_1 - X_1') + c\sqrt{(X_2' - X_2)(X_3' - X_3)} \qquad (1)$$

Table 3—Conditions (T, pH) employed for the calibration curves with the main statistical parameters for each regression curve

T (°C)	pH	Slope	Intercept	R^2adjusted	S.E.	*n*
30	7.2	0.795	9.248	0.974	0.069	50
30	6	0.841	9.279	0.986	0.064	33
30	5.5	0.816	9.006	0.984	0.053	52
30	5	0.864	8.260	0.991	0.132	47
30	4.5	0.763	8.351	0.982	0.043	35
15	7.2	0.815	9.070	0.982	0.064	76
15	6	0.996	8.916	0.996	0.033	62
15	5.5	0.906	8.533	0.993	0.034	58
15	5	1.114	8.531	0.985	0.050	61
15	4.5	1.314	8.349	0.976	0.049	51
10	7.2	0.837	9.044	0.979	0.047	76
10	6	1.009	9.055	0.985	0.047	56
10	5.5	1.033	9.019	0.988	0.044	60
10	5	0.906	8.760	0.963	0.072	47
7	7.2	1.407	9.133	0.985	0.048	60
7	6	1.472	9.020	0.982	0.058	68
7	5.5	1.375	8.896	0.986	0.058	79
4	7.2	1.377	9.037	0.989	0.049	66
4	6	1.242	9.083	0.965	0.076	54

S.E. = Standard error of the slope estimate; n = number of data.

where a, b, and c are the coefficients to be estimated, X_1 is temperature, X_1' the minimum temperature at which growth rate is 0, $X_2 - X_3$ are the concentrations of CA and AA respectively, $X_2' - X_3'$ are the estimated theoretical maximum CA and AA concentrations (% w/v) for organism growth, and μ is the maximum growth rate.

Response surface model (RS). The square-root model was compared with a quadratic response surface model that corresponds to the following equation:

$$y = \beta_0 + \sum_{j=1}^{k} \beta_j X_j + \sum_{j=1}^{k} \beta_{jj} X_j^2 + \sum_{j<1} \sum_{l=2}^{k} \beta_{jl} X_j X_l + \varepsilon \qquad (2)$$

where y is the response variable (μ); β_0 (intercept y-axis) and β_j, β_{jj}, and β_{jl} are the coefficients of the model; X_j and X_l are the independent variables related to the factors (temperature, concentration of CA and concentration of AA, as described in Eq. 1); and ε is the error of the model.

Response surface and square-root models were obtained by fitting the data of Eq. 1 and 2 with the Levenberg-Marquardt algorithm from SPSS 12.0 for Windows™ software.

Hybrid artificial neural networks: adaptive methods for estimating functions. ANN models are commonly based on 1 type of function (sigmoidal or product) to describe data observed; however, in this study, a new methodology is shown for estimating the relation within the independent variables **x** and the dependent variable **y** through linear combinations of sigmoidal and product-base functions. In other words, an estimation of a function with $N - 1$ predicting variables **x** will be performed from a set of data points $\boldsymbol{n}$ or measurements $z_i = (x_i, y_i)$, $(i = 1,\ldots, n)$ in an N-dimensional space:

$$\mathbf{y} = f(\mathbf{x}) + \varepsilon \qquad (3)$$

where ε represents a random error variable with mean 0 and a distribution not known independent of **x**.

Nonparametric adaptive estimation methods are used to obtain a function resulting from a linear combination of base functions, in the form

$$f(\mathbf{x}) = \sum_{j=1}^{M} \beta_j B_j(\mathbf{x}, \mathbf{w_j}) \qquad (4)$$

where $\mathbf{x} = (x_1, x_2, ..., x_p)$ is the vector of input variables, β_j are coefficients of the linear combinations to estimate from the data, $B_j(\mathbf{x}, \mathbf{w_j})$ are base functions, being B_0 (x, p_0) = 1 to introduce this bias into the model, $\mathbf{w_j} = (w_{j1}, w_{j2}, ..., w_{jp})$, are parameters associated with base functions, and M is the number of hidden nodes in the network.

In this paper, 2 base functions, sigmoidal and product, were used individually and in combination.

Product functions (PU) have the following form:

$$B_k(\mathbf{x}, \mathbf{w}_k) = \prod_{i=1}^{p} x_i^{w_{ki}} \quad \mathrm{k} = 1, \ldots, \mathrm{m}_2 \qquad (5)$$

Whereas sigmoidal functions (SU) have the form:

$$B_j(\mathbf{x}, u_\mathbf{j}) = \frac{1}{1 + \exp - \left(u_{j0} + \sum_{i=1}^{p} u_{ji} x_i \right)} \quad \mathrm{j} = 1, \ldots, \mathrm{m}_1; \qquad (6)$$

Thus, the linear combination (hybrid model) to estimate the function (PSU) will be:

$$f(x) = \gamma_0 + \sum_{j=1}^{m_1} \alpha_j B_j(\mathbf{x}, \mathbf{u}_j) + \sum_{k=1}^{m_2} \beta_k B_k(\mathbf{x}, \mathbf{w}_k) \quad (7)$$

where γ_0 is the intercept of the equation, and u_{ji} and α_j are the coefficients of the base functions to be estimated. An example of the structure of hybrid models is shown in Figure 1. The method used consisted of determining a sufficient number of base functions to provide an approach to the function to be estimated (Donoho 1989) so for each $e > 0$ a value of m_1 and m_2 was found, as well as parameter estimators of α_j, β_k, $\hat{\mathbf{u}}_\mathbf{j}$, and $\hat{\mathbf{w}}_k$ for j = 1, . . . , m_1 and k = 1, . . . , m_2 until the following expression was obtained:

$$\left\| f(x) - (\gamma_0 + \sum_{j=1}^{m_1} \alpha_j B_j(\mathbf{x}, \mathbf{u}_j) + \sum_{k=1}^{m_2} \beta_k B_k(\mathbf{x}, \mathbf{w}_k) \right\| < e \quad (8)$$

To overcome this problem, an evolutionary algorithm (EA) will be used as described by Angeline and others (1994) and Hervás-Martinez and others (2006).

The general evolutionary process is based on the use of selection, replication, and mutation operators (parametric and structural). Evolution of the network topology corresponds to a local search for the structure of sigmoidal and product-base functions that display the best fit to the training data points, determining the values of the m_1 and m_2 associated with the number of base functions considered. On the other hand, evolution of the network weights is related to the vectors $\mathbf{u}_\mathbf{j}$ and $\mathbf{w}_\mathbf{k}$ that determine coefficients presented in each base function, and those that result from linear combinations of these base functions (α_j, β_k). The general structure of the evolutionary algorithm, which is described in detail in Hervás-Martinez and others (2006), is applied to an initial population of N individuals. It can be supported in the following steps:

1. Generate initial population with randomly generated networks.
2. Evaluate the fitness score for each individual of the population based on the objective function.
3. Copy the best individual to the next generation.
4. The best 10% of the population substitutes the worst 10%.
5. Apply parametric mutation operators to the best 10% of the population.
6. Apply structural parametric mutation to the rest of the population.

The values of parameters used by the evolutionary algorithm for PUNN are shown in Table 4. It should be pointed out that the algorithm is quite robust to the modification of these parameters. The EA begins generating N networks randomly, choosing the total number of hidden nodes from a uniform distribution in the interval $(0, M]$, where $m_1 + m_2 = M$ corresponds to the maximum number of hidden nodes in each network. The number of connections between nodes from the hidden and input layers is determined from a uniform distribution in the interval $(0, p]$, where p represents the number of independent variables.

Once the network topology is defined, 1 weight is assigned to each connection from a uniform distribution in the interval $[-L, L]$ for the weights between the hidden and input layer and $[-U, U]$ for the weights between the hidden and the output layer.

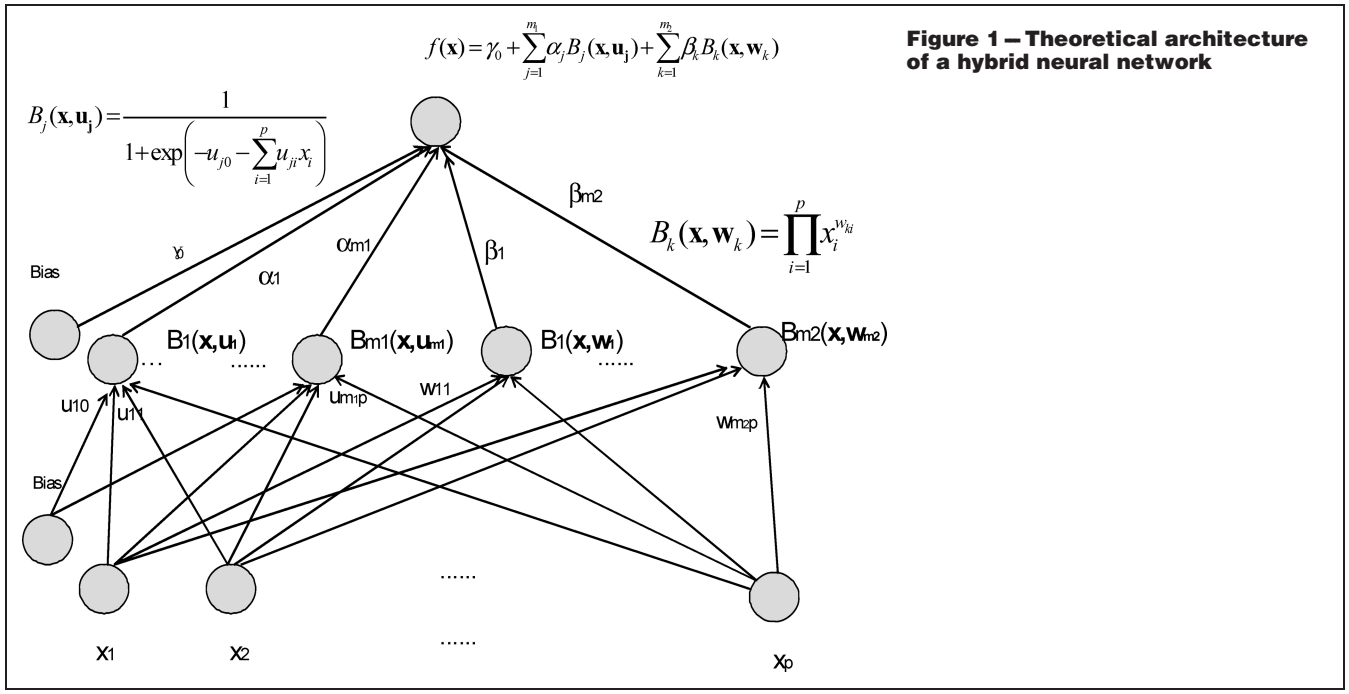

Figure 1 — Theoretical architecture of a hybrid neural network

Table 4 — Parametric values used by the evolutionary algorithm for product unit neural networks for the estimation of *Listeria monocytogenes*

Population parameters		Structural mutation parameters: interval [Δ_M, Δ_M]		Parametric mutation parameters of Eq. (9)	
Size, N_P	1000	add nodes	[1, 2]	$\alpha_1(0)$	1
Maximum number of hidden nodes, p	8	delete nodes	[1, 2]	$\alpha_2(0)$	5
Number of independent variables, k	4	add connections	[1, 6]	β	0.5
Exponent interval, $[-M, M]$	[0, 3]	delete connections	[1, 6]	R	10
Coefficient interval, $[0, L]$	[−5, 5]				

There are 2 types of mutations in an EA: parametric and structural. The severity of these mutations depends on the temperature $T(R)$ of the network model, defined as:

$$T(R) = 1 - A(R)\ , \quad 0 \le T(R) \le 1 \tag{9}$$

where the aptitude $A(R)$ of a network R is calculated as a decreasing function of the root mean square error $E(R)$ from the expression

$$A(R) = \frac{1}{1 + E(R)}, \quad 0 < A(R) \le 1 \tag{10}$$

Parametric mutation is applied to the 10% of the selected networks that present the best fit and affect the network weights. Parametric mutation consists of adding to the coefficients α_j, β_k, a random variable of mean 0, and standard deviation $\alpha_1(t)T(R)$, while the coefficients u_{ji} and w_{ki} present a random variable of mean 0 and standard deviation $\alpha_2(t)T(R)$, where $\alpha_1(t) \ll \alpha_2(t)$, $\forall t$. Mutations of the weights u_{ji} and w_{ki} corresponding to the exponents of functions to be modeled should be less severe than mutations in the weights α_j, β_k, corresponding to the base-function coefficients.

Structural mutation that affects network topology (hidden nodes and connections) was applied to the 90% of the networks that presented the worst fit to the training data points. Five types of structural mutations were used in this study: add nodes, eliminate nodes, add connections, eliminate connections, and join nodes.

All independent variables and the dependent variable considered in the ANN models were scaled in the rank [0.1, 0.9] as per the following example using temperature T:

$$T^* = 0.8\frac{T - T_{\min}}{T_{\max} - T_{\min}} + 0.1 \tag{11}$$

where T is the original temperature, $T_{\min}$ and $T_{\max}$ are the minimum and maximum values of the dataset, and T^* is the scaled temperature. Once obtained, model estimations should be descaled following the same equation.

Evaluation criteria. To evaluate the magnitude of the difference between the observed and predicted values of the different models proposed, root mean-square error (RMSE) and standard error of prediction (SEP) (Hervás and others 2001) were applied to both the training and generalization datasets. These values are defined by:

$$\mathrm{RMSE} = \frac{\sqrt{\sum (\mu pred - \mu obs)^2}}{n} \tag{12}$$

$$\mathrm{SEP} = \frac{100}{\overline{\mu}_{obs}}\sqrt{\frac{\sum_{i=1}^{n} (\mu_{pred} - \mu_{obs})^2}{n}} \tag{13}$$

where μ_{obs} is the observed maximum specific growth rate, μ_{pred} is the predicted specific growth rate, and n the number of data.

SEP is a relative percentage that explains the deviations between predictions and observations, and is independent of the size of the values for the dependent variable.

For model validation, the bias factor (B_f) and accuracy factor (A_f) (Ross 1996) were applied to the generalization dataset and are represented in the following equations:

$$B_f = 10^{\left(\sum \log(\mu pred/\mu obs)/n\right)} \tag{14}$$

$$A_f = 10^{\left(\sum \log(\mu pred/\mu obs)/n\right)} \tag{15}$$

Results and Discussion

The experimental data used in this study encompassed 157 growth conditions of *L. monocytogenes* (95 conditions selected for the training and 62 for generalization dataset with 5 replicates per condition) in modified TSB as a function of storage temperature (4 to 30 °C), CA (0% to 0.4% w/v) and AA (0% to 0.4% w/v). All possible combinations were tested, but only conditions in which growth was observed were considered in the analysis procedure. Conditions selected are represented in Table 5 and 6.

Primary model

Log-absorbance data were transformed into cell counts (log CFU/mL) using the calibration curves obtained previously (Table 2). Later, the Baranyi model (Baranyi and Roberts 1994) was fitted to cell count data using DMFit 1.0. Based on this primary model, μ was estimated from cell count data.

The Baranyi model presented a good fit to the data observed, corroborating the observations of other authors (George and others 1996; McClure and others 1997). Figure 2 shows a growth curve of cell count data fitted to Baranyi model. It should be noted that some extrapolation was made when starting from absorbance data. Membré and others (1999) compared this adjustment to the one given using the Gompertz equation and found significant differences in growth rate estimation. They concluded that the 1st model provided a better goodness-of-fit.

Secondary models

The 2nd step was to find the relationship between growth rate and environmental parameters. Five different model approaches were used to obtain predicted *L. monocytogenes* growth rate: RS model, SR model, and 3 ANN models (PU, SU, and PSU).

For the RS model, different transformations of μ were tested, and $\sqrt{\mu}$ was chosen to stabilize the variance of the data. Subsequently, a linear regression procedure with a stepwise method was used to link $\sqrt{\mu}$ with the environmental factors considered in the model. The final equation was:

$$\begin{aligned}\sqrt{\mu} = {} & 0.018 - 1.353(\mathrm{CA}^2) - 0.285(\mathrm{AA}^2) + 0.021(\mathrm{T}) \\ & -0.027(\mathrm{T})\ (\mathrm{CA}) - 0.010(\mathrm{T})\ (\mathrm{AA}) - 0.899(\mathrm{CA})\ (\mathrm{AA})\end{aligned} \tag{16}$$

The minimal parameter values (T′, CA′, and AA′) were estimated to fit the SR model to the data observed. These values are shown in Table 7 along with their lower and upper confidence intervals, and were obtained by extrapolating conditions at which μ was zero. The secondary model was obtained in the same way as described above.

$$\sqrt{\mu} = -0.755 + 0.016(\mathrm{T} - \mathrm{T}') + 1.315\sqrt{(\mathrm{CA}' - \mathrm{CA})\ (\mathrm{AA}' - \mathrm{AA})} \tag{17}$$

Finally, the neural network models were adjusted by repeating the algorithm to obtain the architecture that best fits the data observed.

The structure of the interconnected neurons in a neural network depends on the complexity of a given problem. The number of neurons in the input and the output layers is determined by the number of input and output variables in the problem. The number of neurons in the hidden layers is related to the performance of a neural network. Too few hidden neurons limit the ability of the network to model the problem, and too many result in overtraining of the input/output pair patterns presented in the training process. This demonstrates the need to develop methods that enable the number of parameters to be reduced without significantly diminishing the

Table 5—Conditions selected for the training dataset and observed/predicted mean values of the 5 replicates/condition of maximum growth rate (μ) from the different models

T (°C)	CA% (w/v)	AA% (w/v)	$\overline{\mu}_{OBS}$	Predicted values				
				$\overline{\mu}_{RS}$	$\overline{\mu}_{SR}$	$\overline{\mu}_{PU}$	$\overline{\mu}_{SU}$	$\overline{\mu}_{PSU}$
30	0	0	0.417	0.424	0.407	0.413	0.417	0.401
30	0	0.1	0.324	0.381	0.345	0.369	0.375	0.355
30	0	0.2	0.329	0.334	0.285	0.327	0.332	0.313
30	0	0.3	0.281	0.285	0.227	0.285	0.289	0.273
30	0	0.4	0.247	0.233	0.171	0.241	0.246	0.233
30	0.1	0	0.355	0.311	0.297	0.320	0.314	0.320
30	0.1	0.1	0.294	0.265	0.249	0.276	0.271	0.279
30	0.1	0.2	0.230	0.218	0.204	0.235	0.228	0.240
30	0.1	0.3	0.239	0.171	0.160	0.192	0.186	0.196
30	0.1	0.4	0.105	0.125	0.118	0.148	0.144	0.145
30	0.2	0	0.231	0.191	0.193	0.220	0.211	0.218
30	0.2	0.1	0.210	0.149	0.160	0.176	0.169	0.171
30	0.2	0.2	0.092	0.108	0.128	0.134	0.127	0.120
30	0.2	0.3	0.041	0.071	0.098	0.092	0.088	0.074
30	0.3	0	0.079	0.084	0.098	0.115	0.112	0.094
30	0.3	0.1	0.052	0.053	0.079	0.071	0.072	0.051
30	0.3	0.2	0.011	0.027	0.061	0.029	0.035	0.020
30	0.3	0.3	0.011	0.008	0.045	0.001	0.001	0.001
30	0.3	0.4	0.012	0.000	0.029	0.001	0.001	0.001
25	0	0	0.314	0.298	0.308	0.293	0.314	0.321
25	0	0.1	0.235	0.267	0.255	0.260	0.272	0.284
25	0	0.2	0.242	0.233	0.204	0.229	0.232	0.244
25	0	0.3	0.220	0.196	0.155	0.196	0.194	0.197
25	0	0.4	0.139	0.158	0.110	0.163	0.158	0.148
25	0.1	0	0.231	0.217	0.214	0.213	0.213	0.233
25	0.1	0.1	0.228	0.183	0.174	0.180	0.175	0.184
25	0.1	0.2	0.152	0.148	0.136	0.148	0.140	0.139
25	0.1	0.3	0.109	0.113	0.101	0.116	0.106	0.105
25	0.1	0.4	0.055	0.079	0.068	0.083	0.076	0.079
25	0.2	0	0.067	0.128	0.127	0.127	0.121	0.117
25	0.2	0.1	0.113	0.097	0.101	0.094	0.088	0.086
25	0.2	0.2	0.049	0.068	0.076	0.062	0.057	0.063
25	0.2	0.3	0.025	0.041	0.053	0.030	0.030	0.043
25	0.3	0	0.031	0.050	0.054	0.038	0.039	0.047
25	0.3	0.1	0.024	0.028	0.040	0.005	0.012	0.028
20	0	0	0.196	0.224	0.194	0.196	0.210	0.216
20	0	0.1	0.159	0.179	0.174	0.173	0.179	0.171
20	0	0.2	0.149	0.136	0.150	0.150	0.150	0.137
20	0	0.3	0.129	0.097	0.125	0.127	0.125	0.112
20	0	0.4	0.123	0.062	0.098	0.103	0.101	0.092
20	0.1	0	0.140	0.144	0.139	0.141	0.139	0.122
20	0.1	0.1	0.119	0.112	0.116	0.118	0.114	0.100
20	0.1	0.2	0.107	0.082	0.092	0.096	0.091	0.082
20	0.1	0.3	0.074	0.055	0.067	0.073	0.070	0.066
20	0.1	0.4	0.034	0.032	0.044	0.049	0.051	0.052
20	0.2	0	0.096	0.075	0.078	0.083	0.079	0.067
20	0.2	0.1	0.068	0.055	0.057	0.060	0.059	0.052
20	0.2	0.2	0.030	0.037	0.037	0.037	0.041	0.039
20	0.2	0.3	0.011	0.022	0.019	0.014	0.025	0.027
20	0.3	0	0.023	0.022	0.025	0.023	0.029	0.027
20	0.3	0.1	0.038	0.014	0.012	0.001	0.014	0.016
15	0	0	0.109	0.153	0.112	0.116	0.116	0.114
15	0	0.1	0.083	0.116	0.100	0.101	0.097	0.097
15	0	0.2	0.104	0.082	0.086	0.087	0.081	0.083
15	0	0.3	0.071	0.053	0.069	0.072	0.066	0.070
15	0	0.4	0.059	0.028	0.052	0.056	0.053	0.058
15	0.1	0	0.079	0.089	0.079	0.083	0.076	0.071
15	0.1	0.1	0.063	0.064	0.064	0.068	0.062	0.059
15	0.1	0.2	0.057	0.042	0.049	0.054	0.049	0.048
15	0.1	0.3	0.063	0.023	0.033	0.039	0.038	0.038
15	0.1	0.4	0.032	0.009	0.019	0.024	0.028	0.029
15	0.2	0	0.038	0.037	0.040	0.048	0.044	0.037
15	0.2	0.1	0.034	0.026	0.027	0.033	0.034	0.028
15	0.2	0.2	0.014	0.012	0.015	0.019	0.024	0.020
15	0.3	0	0.015	0.004	0.009	0.011	0.020	0.011
10	0	0	0.047	0.095	0.052	0.054	0.053	0.062
10	0	0.1	0.037	0.067	0.047	0.046	0.043	0.053
10	0	0.2	0.037	0.042	0.039	0.039	0.035	0.044
10	0	0.3	0.022	0.022	0.030	0.031	0.027	0.036
10	0	0.4	0.016	0.007	0.020	0.023	0.021	0.029
10	0.1	0	0.026	0.046	0.036	0.038	0.033	0.034
10	0.1	0.1	0.018	0.029	0.028	0.030	0.026	0.027
10	0.1	0.2	0.007	0.015	0.019	0.023	0.019	0.020
10	0.1	0.3	0.001	0.005	0.011	0.015	0.014	0.014
10	0.1	0.4	0.001	0.000	0.004	0.007	0.009	0.009
10	0.2	0	0.008	0.012	0.015	0.021	0.018	0.013
7	0	0	0.030	0.027	0.027	0.027	0.030	0.038
7	0	0.1	0.024	0.024	0.024	0.023	0.023	0.031
7	0	0.2	0.019	0.024	0.020	0.018	0.018	0.024
7	0	0.3	0.016	0.010	0.014	0.014	0.013	0.018
7	0	0.4	0.014	0.001	0.008	0.009	0.009	0.013
7	0.1	0	0.025	0.028	0.018	0.019	0.017	0.016
7	0.1	0.1	0.015	0.015	0.013	0.014	0.012	0.011
7	0.1	0.2	0.008	0.005	0.008	0.010	0.008	0.006
7	0.2	0	0.008	0.004	0.006	0.010	0.007	0.000
4	0	0	0.018	0.044	0.011	0.008	0.014	0.018
4	0	0.1	0.011	0.025	0.009	0.006	0.010	0.013
4	0	0.2	0.006	0.011	0.007	0.005	0.006	0.008
4	0	0.3	0.003	0.002	0.004	0.003	0.003	0.003
4	0	0.4	0.004	0.000	0.002	0.001	0.001	0.001
4	0.1	0	0.014	0.004	0.006	0.005	0.006	0.001
4	0.1	0.1	0.006	0.005	0.004	0.004	0.003	0.001
4	0.1	0.2	0.007	0.001	0.002	0.002	0.000	0.001
4	0.1	0.3	0.001	0.001	0.000	0.000	0.001	0.001

T = temperature; CA = citric acid concentration; AA = ascorbic acid concentration; μ_{OBC} = observed values of μ; SR = square-root model; RS = response surface model; PU = product-base unit function; SU = sigmoidal-base unit function; PSU = hybrid model.

model's estimation capacity (Hervás and others 2001). The architecture for the best networks chosen is displayed in the following equations. All variables (T^*, CA^*, AA^*, and μ^*) were scaled in the rank (0.1 to 0.9).

PU model:

$$\mu^* = 0.098 - 0.963(T^{*1.682})(CA^{*1.086}) + 2.887(T^{*30.026})(CA^{*1.010}) + 0.974(T^{*1.724})(AA^{*-0.020}) - 0.405(T^{*1.449})(AA^{*1.146}) \quad (18)$$

SU model:

$$\mu^* = 2.175 - \frac{0.692}{[1 + e^{-[-6.810+8.421(T^*)+0.570(CA^*)]}]} - \frac{2.102}{(1 + e^{-[3.935-5.099(T^*)+1.235(CA^*)+0.768(AA^*)]})} \quad (19)$$

PSU model:

$$\mu^* = 0.153 - 0.553[(T^*)^{3.235}(CA^*)^{-0.155}(AA^*)^{0.019}] - \frac{0.132}{(1 + e^{-[12.945-25.315(T^*)+11.009(CA^*)+6.406(AA^*)]})} + \frac{3.621}{(1 + e^{-[-3.619+3.473(T^*)-1.211(CA^*)-0.467(AA^*)]})} \quad (20)$$

By applying the corresponding equations, predicted values for μ were obtained. Table 5 and 6 show the predictions of the average of μ for the 5 models considered for both training and generalization datasets.

Evaluation of the goodness-of-fit

The goodness-of-fit of the training and generalization datasets for the models considered were evaluated by calculating RMSE and SEP, and are shown in Table 8.

In all cases, the models developed produced relatively low values for RMSE (< 0.0318), which means that the observed and predicted growth rates were very similar. However, for the generalization dataset, RMSE values were lower for the ANN models performed. These results support the findings of other authors. Yu and others (2006) compared nonlinear regression models with ANNs. From all the models presented, ANN displayed the best RMSE, demonstrating its capacity to generate more accurate predictions than RS models. Esnoz and others (2006) offered a comparison between RS models and neural network models for predicting *Bacillus stearothermophilus* inactivation rate. The RS model achieved an RMSE of 0.19 to experimental data, higher than that obtained using ANN models, which ranged between 0.13 and 0.16. García-Gimeno and others (2005) obtained an RMSE of between 0.006 and 0.115. These values are similar to the errors observed in other ANN models (Hajmeer and others 1997; Lou and Nakai, 2001; García-Gimeno and others 2003) or in RS models (Juneja and others 2001; Zurera-Cosano and others 2004).

Table 6—Conditions selected for the generalization dataset and observed/predicted mean values of the 5 replicates/condition of μ from the different models

T (°C)	CA% (w/v)	AA% (w/v)	$\overline{\mu}_{OBS}$	Predicted values				
				$\overline{\mu}_{RS}$	$\overline{\mu}_{SR}$	$\overline{\mu}_{PU}$	$\overline{\mu}_{SU}$	$\overline{\mu}_{PSU}$
30	0.00	0.05	0.407	0.403	0.376	0.390	0.396	0.377
30	0.05	0.05	0.354	0.360	0.340	0.359	0.357	0.359
30	0.05	0.00	0.345	0.369	0.351	0.368	0.366	0.368
25	0.05	0.15	0.206	0.241	0.191	0.205	0.204	0.220
25	0.05	0.25	0.180	0.180	0.148	0.173	0.167	0.171
25	0.05	0.35	0.097	0.143	0.107	0.141	0.132	0.129
25	0.15	0.05	0.126	0.152	0.152	0.154	0.148	0.148
25	0.15	0.15	0.071	0.129	0.120	0.122	0.113	0.110
25	0.15	0.25	0.065	0.096	0.090	0.090	0.082	0.083
25	0.15	0.35	0.014	0.066	0.063	0.057	0.052	0.061
25	0.25	0.05	0.029	0.070	0.078	0.066	0.063	0.065
25	0.00	0.05	0.298	0.241	0.282	0.276	0.293	0.302
25	0.05	0.05	0.252	0.251	0.241	0.240	0.247	0.268
25	0.05	0.00	0.244	0.256	0.260	0.254	0.263	0.284
20	0.05	0.15	0.134	0.159	0.126	0.135	0.132	0.119
20	0.05	0.25	0.099	0.114	0.091	0.112	0.107	0.098
20	0.05	0.35	0.054	0.088	0.060	0.089	0.085	0.081
20	0.15	0.05	0.086	0.094	0.095	0.101	0.096	0.083
20	0.15	0.15	0.049	0.079	0.070	0.078	0.074	0.067
20	0.15	0.25	0.055	0.056	0.048	0.055	0.055	0.052
20	0.15	0.35	0.015	0.035	0.028	0.032	0.038	0.039
20	0.25	0.05	0.022	0.038	0.039	0.041	0.044	0.039
20	0.25	0.15	0.014	0.026	0.026	0.019	0.027	0.027
20	0.00	0.05	0.180	0.152	0.201	0.184	0.194	0.193
20	0.05	0.05	0.146	0.163	0.163	0.157	0.159	0.146
20	0.05	0.00	0.154	0.166	0.183	0.169	0.173	0.164
15	0.20	0.25	0.009	0.008	0.042	0.011	0.020	0.016
15	0.05	0.15	0.080	0.074	0.063	0.078	0.071	0.071
15	0.30	0.05	0.009	0.003	0.019	0.004	0.015	0.008
15	0.05	0.25	0.045	0.048	0.049	0.063	0.057	0.059
15	0.05	0.35	0.066	0.027	0.046	0.048	0.046	0.048
15	0.15	0.05	0.063	0.051	0.051	0.058	0.053	0.047
15	0.15	0.15	0.084	0.033	0.041	0.044	0.041	0.038
15	0.15	0.25	0.028	0.018	0.027	0.029	0.031	0.029
15	0.15	0.30	0.037	0.012	0.019	0.022	0.026	0.025
15	0.25	0.05	0.021	0.013	0.017	0.022	0.026	0.019
15	0.25	0.10	0.013	0.009	0.013	0.015	0.022	0.015
15	0.00	0.05	0.095	0.134	0.088	0.108	0.106	0.105
15	0.05	0.05	0.096	0.104	0.094	0.092	0.086	0.084
15	0.05	0.00	0.083	0.119	0.096	0.100	0.095	0.091
10	0.05	0.05	0.046	0.057	0.053	0.042	0.038	0.043
10	0.05	0.15	0.050	0.036	0.035	0.035	0.030	0.035
10	0.05	0.25	0.028	0.019	0.027	0.027	0.023	0.028
10	0.05	0.35	0.011	0.007	0.018	0.019	0.017	0.021
10	0.15	0.05	0.009	0.021	0.020	0.026	0.022	0.019
10	0.15	0.15	0.032	0.010	0.015	0.018	0.016	0.014
7	0.05	0.05	0.023	0.036	0.020	0.021	0.020	0.023
7	0.05	0.15	0.017	0.020	0.018	0.016	0.015	0.017
7	0.05	0.25	0.007	0.008	0.012	0.012	0.010	0.012
7	0.05	0.35	0.006	0.001	0.007	0.008	0.007	0.007
7	0.15	0.05	0.006	0.009	0.009	0.012	0.009	0.005
7	0.00	0.05	0.024	0.055	0.023	0.025	0.026	0.034
7	0.00	0.15	0.023	0.033	0.023	0.020	0.020	0.028
7	0.00	0.25	0.021	0.016	0.018	0.016	0.015	0.021
7	0.00	0.35	0.013	0.004	0.012	0.012	0.011	0.016
7	0.05	0.00	0.026	0.046	0.021	0.023	0.023	0.026
7	0.05	0.10	0.019	0.028	0.020	0.019	0.017	0.020
7	0.05	0.20	0.011	0.013	0.015	0.014	0.012	0.015
7	0.05	0.30	0.008	0.004	0.010	0.010	0.008	0.010
4	0.00	0.05	0.012	0.034	0.010	0.007	0.012	0.015
4	0.05	0.00	0.011	0.027	0.009	0.007	0.009	0.009

T = temperature; CA = citric acid concentration; AA = ascorbic acid concentration; μ_{OBC} = observed values of maximum growth rate (μ); SR = square-root model; RS = response surface model; PU = product-base unit function; SU = sigmoidal-base unit function; PSU = hybrid model.

Since RMSE values depend on the magnitude of the data, SEP values were calculated because they are relative percentages that provide better comparisons between different models. The SEP values were acceptable for all models presented, but produced considerably lower values for the PU, SU, and PSU models (< 24.23% for both training and generalization datasets, according to Table 8). In this study, ANN models presented a better generalization capacity compared to RS and SR models. Several authors highlight that SU models produce better estimations of kinetic parameters than other models such as the RS (Hajmeer and others 1997; Hervás and others 2001; Lou and Nakai 2001). García-Gimeno and others (2002) observed SEP values that were lower than 22% for predictions of *Lactobacillus plantarum* growth rate and which were much better than the RS model (35.6%), so SU models were chosen instead of RS models based on the lower SEP, despite the fact that the SU models had a greater degree of complexity. Although some researchers do not agree with the use of ANN to predict growth parameters due to their complexity, other studies have confirmed that SU models could be even simpler than regression in certain cases (Hervás and others 2001; García-Gimeno and others 2002). Geeraerd and Van Impe (1999) extended neural networks to model the specific growth rate of *Shigella flexneri* in BHI medium as a function of temperature, pH, NaCl, and $NaNO_2$, and compared ANNs with polynomial models. They found a better performance for ANN models. Cheroutre-Vialette and Lebert (2000) developed a recurrent neural network for the prediction of *L. monocytogenes* growth under variable conditions. However, a better performance was obtained against an increase in the number of parameters to be estimated.

In this study, out of the PU, SU, and PSU models, as shown in Table 8, the SU model presented the best performance to describe growth rate data. The use of PU and PSU would be very valuable if a strong interaction existed *a priori* between the factors that affect the prediction of microbe growth parameters. However, PU and PSU models were not suitable in comparison with the other models because they produced an excessive number of parameters without improving generalization capacity. This demonstrates the need to develop alternative methods that would decrease the number of parameters required without diminishing performance (Hervás and others 2000). A few methods have already been developed to eliminate unnecessary weights or parameters. García-Gimeno and others

Table 7—Cardinal values of the SR model with upper and lower confidence intervals (C.I.)

	Coefficient	95% lower C.I.	95% upper C.I.
T′	−0.740	−1.925	0.583
CA′	0.502	0.396	0.757
AA′	0.905	0.479	1.437

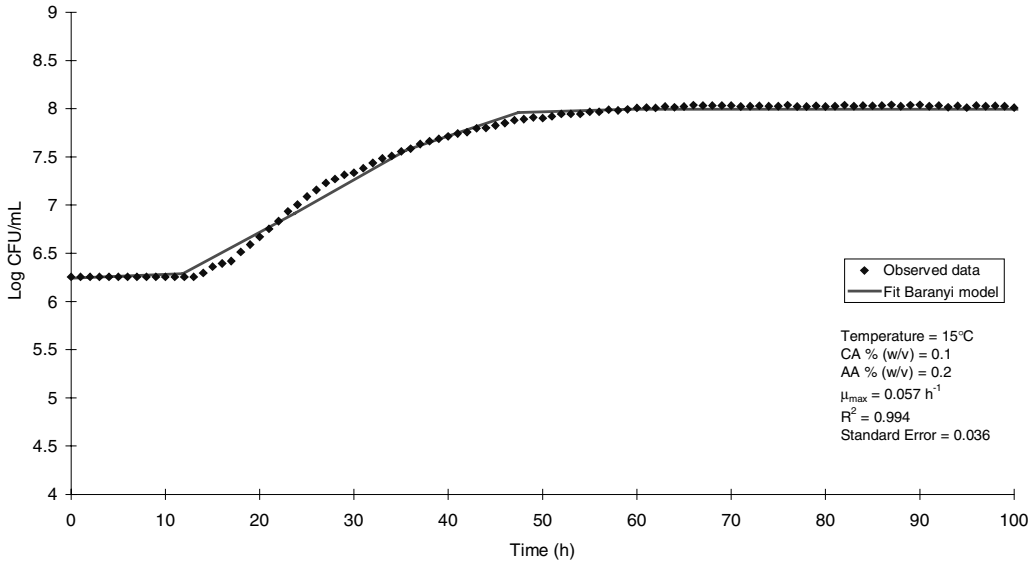

Figure 2—Growth curve of *Listeria monocytogenes* based on cell count data fitted to Baranyi model

(2002) used a pruning algorithm, removing unnecessary weights and neurons during the training process without losing generalization capacity. There are several different pruning methods: one of the most commonly used methods involves designing an ANN using evolutionary algorithms (Hervás and others, 2001). In our study, EA pruning was carried out to reduce complexity. The number of parameters for each model is expressed in Table 8. The SU model used fewer parameters (10) in comparison with the PU (13) and PSU (15) models, and also provided a better fit to the data observed. Hervás and others (2006) compared SU and PU models with RS models to predict kinetic parameters for *Leuconostoc mesenteroides*. They concluded that the RS model was better for predicting growth rate since it used fewer parameters, whereas PU models were more suitable for predicting lag time and maximum population density, since they presented a lower error of prediction.

Mathematical validation

In order to determine the performance of the models, the calculated values for B_f and A_f are shown for the generalization dataset (Table 8). B_f is related to the position of the data points (above or below) with regard to the line of equivalence (structural deviation). A_f, on the other hand, provides information about the mean distance between each data point and the line of equivalence.

B_f is slightly above 1 for all models, but more accurate values were obtained using the RS and SR models. This means that the model overestimates μ (predictive μ > observed μ), so predictions will be fail-safe. However, as Ross (1999) stated, growth models of pathogenic microorganisms should present values for B_f of between 0.9 and 1.15. Since all B_f values were lower than 1.15, the models proposed presented an acceptable bias.

A_f values were above 1 for all models, but in this case, the neural network models presented more accurate values (1.34 to 1.36). However, Ross and others (2000) considered A_f values of up to 0.15 (15%) for each factor included in the model. Therefore, in our study, using 3 factors (temperature, CA, and AA), A_f values of up to 1.45 should be expected. Since A_f values were lower, except for the SR model, which was slightly higher, the models provide acceptable descriptions of the data observed. Carrasco and others (2006) obtained similar values for A_f and B_f when validating a model describing *L. monocytogenes* growth rate (1.16 and 1.05, respectively). Lebert and others (2000) observed a good fit when they applied mathematical validation to models to estimate generation time for *Pseudomonas* spp. ($B_f = 0.82$ to 1.16 and $A_f = 1.13$ to 1.24). In a different study on the same microorganism, similar values were obtained ($B_f = 0.84$; $A_f = 1.23$) (Neumeyer and others 1997).

Validation of the models was proven with external data from scientific literature in Table 9. B_f and A_f for each model were calculated. As described in Table 9, the models developed in this study shown an adequate generalization capacity, since B_f values were near 1, except for the SR model. On the other hand, A_f values were slightly above 1, and SU model provided the best A_f value (1.285). There are very few reports that include CA or AA, alone or in combination, as preservatives to inhibit *L. monocytogenes* growth. Therefore, further validation should be performed on foods in which both organic acids are present to enable the application of the models in food industries.

Conclusions

In this study, different secondary modeling approaches (RS, SR, and 3 ANN models) were presented for estimating growth

Table 8—Evaluation criteria for each model performed: Number of parameters, root mean square error (RMSE), standard error of prediction (SEP), accuracy factor (A_f) and bias factor (B_f)

		Training data		Generalization data			
Model	No. parameters	RMSE	SEP (%)	RMSE	SEP (%)	B_f	A_f
Response surface	6	0.0222	24.59	0.0303	38.65	1.09	1.41
Square root	3	0.0318	34.04	0.0238	29.03	1.02	1.56
PU (3:4:1)	13	0.0230	23.29	0.0193	24.23	1.11	1.35
SU (3:2:1)	10	0.0225	22.41	0.0182	23.05	1.14	1.36
PSU (3:3:1)	15	0.0226	24.19	0.0190	23.92	1.14	1.33

Table 9—Validation of each model performed with data from scientific literature

Reported values				Predicted values				
T (°C)	CA% (w/v)	AA% (w/v)	μ_{max} (h^{-1})	μ_{RS} (h^{-1})	μ_{SR} (h^{-1})	μ_{PU} (h^{-1})	μ_{SU} (h^{-1})	μ_{PSU} (h^{-1})
7	0.050	0	0.021[a]	0.023	0.044	0.023	0.023	0.026
13	0.050	0	0.064[a]	0.073	0.094	0.076	0.070	0.072
13	0.100	0	0.040[a]	0.059	0.067	0.063	0.056	0.055
21	0.050	0	0.176[a]	0.183	0.188	0.185	0.191	0.189
21	0.100	0	0.078[a]	0.151	0.149	0.155	0.153	0.138
5.5	0	0	0.018[b]	0.018	0.053	0.016	0.021	0.027
10.5	0	0	0.057[b]	0.057	0.097	0.059	0.058	0.067
15	0	0	0.120[b]	0.111	0.147	0.116	0.116	0.114
20	0	0	0.188[b]	0.224	0.194	0.196	0.210	0.216
25	0	0	0.301[b]	0.299	0.308	0.293	0.314	0.321
4	0.138	0	0.003[c]	0.004	0.006	0.004	0.003	0.001
10	0.095	0	0.045[c]	0.036	0.046	0.039	0.034	0.035
4	0	0.120	0.023[c]	0.009	0.021	0.006	0.009	0.012
10	0	0.120	0.048[c]	0.045	0.059	0.045	0.041	0.051
4	0	0.011	0.032[c]	0.010	0.041	0.008	0.013	0.017
10	0	0.011	0.049[c]	0.051	0.089	0.053	0.052	0.061
			B_f	0.958	1.445	0.929	0.965	0.982
			A_f	1.310	1.461	1.379	1.285	1.372

[a]Ahamad and Marth (1989).
[b]Nyati (2000).
[c]Giannuzzi and Zaritzky (1996).
T = temperature; CA = citric acid concentration; AA = ascorbic acid concentration; μ_{max} = reported values of maximum growth rate (μ); SR = square-root model; RS = response surface model; PU = product-base unit function; SU = sigmoidal-base unit function; PSU = hybrid model; A_f = accuracy factor; and B_f = bias factor.

parameters (μ). In general, the ANN models were found to yield a better fit with experimentally measured data in comparison with the data predicted by the RS and SR models. This justifies its use in the field of predictive microbiology. In this study, given that only 3 factors (temperature, CA, and AA) were used, the model is not excessively complex, so a simpler ANN model based on a sigmoidal function provided acceptable estimations for *L. monocytogenes* growth rate with a better goodness-of-fit and generalization capacity than the RS or SR models.

The results obtained in this study showed that more complex models imply a better fit to data observed than regression models. However, simpler models provide good solutions in certain cases, especially when few environmental factors are taken into account. The balance between generalization properties and the ease of use is the main consideration when applying secondary modeling approaches to achieve accurate predictions about the behavior of microorganisms.

Acknowledgments

This work was partly financed by the Ministry of Education and Science (MEC) AGL2005-0119 (Dept. of Food Science, Univ. of Cordoba) and TIN2005-08386-C05-02 (Dept. of Computer Science, Univ. of Cordoba) projects. Additional funding was also provided by FEDER and a grant from MEC.

References

Ahamad N, Marth EH. 1989. Behaviour of *Listeria monocytogenes* at 7, 13, 21 and 35°C in trypose broth acidified with acetic, citric or lactic acid. J Food Prot 52:688–95.
Angeline PJ, Saunders GM, Pollack JB. 1994. An evolutionary algorithm that constructs recurrent neural networks. IEEE Trans Neural Netw 5(1):54–65.
Baranyi J, Roberts TA. 1994. A dynamic approach to predicting bacterial growth in food. Int J Food Microbiol 23:277–94.
Buchanan RL, Golden MH. 1994. Interaction of citric acid concentration and pH on the kinetics of *Listeria monocytogenes* inactivation. J Food Prot 57:567–70.
Buchanan RL, Phillips JG. 1993. Response surface model for predicting the effects of temperature, pH, sodium chloride content, sodium nitrite concentration, and atmosphere on the growth of *Listeria monocytogenes*. J Food Prot 53:370–6.
Carrasco E, García-Gimeno R, Seselovsky R, Valero A, Pérez F, Zurera G, Todd E. 2006. Predictive model of *Listeria monocytogenes*` growth rate under different temperatures and acids. Food Sci Technol Int 12:47–57.
Cheroutre-Vialette M, Lebert A. 2000. Modelling the growth of *Listeria monocytogenes* in dynamic conditions. Int J Food Microbiol 55:201–7.
Cheroutre-Vialette M, Lebert A. 2002. Application of recurrent neural network to predict bacterial growth in dynamic conditions. Int J Food Microbiol 73:107–18.
Cohen S, Intrator N. 2002. Forward and backward selection in regression hybrid network, Multiplier Classifier Systems: Third International Workshop, MCS Cagliary (Italy), June 24-26. Vol. 2364, 98. Heidelberg: Springer Berlin.
Cohen S, Intrator A. 2005. Hybrid projection-based and radial basis function architecture: initial values and global optimisation, pattern analysis & applications. pp 113–20.
Dalgaard P, Mejlholm O, Huss HH. 1997. Application of an iterative approach for development of a microbial model predicting the shelf-life of packed fish. Int J Food Microbiol 38:169–79.
Devlieghere F, Geeraerd AH, Versyck KJ, Bernaert H, Van Impe JF, Debevere J. 2000. Shelf-life of modified atmosphere packed cooked meat products: addition of Na-lactate as a fourth shelf-life alternative determinative factor in a model and product validation. Int J Food Microbiol 58:93–106.
Devlieghere F, Geeraerd AH, Versyck KJ, Van De Waetere B, Van Impe JF, Debevere J. 2001. Growth of *Listeria monocytogenes* in modified atmosphere packed cooked meat products: a predictive model. Food Microbiol 18:53–66.
Donoho D. 1989. Projection based in approximation and a duality with kernel methods. Ann Statist 17:58–106.
Eddy BP, Ingram M. 1953. Interaction between ascorbic acid and bacteria. Bacteriol Rev 17:93–107.
Esnoz A, Periago PM, Conesa R, Palop A. 2006. Application of artificial neural networks to describe the combined effect of pH and NaCl on the heat resistance of *Bacillus stearothermophilus*. Int J Food Microbiol 106:153–8.
Francois K, Devlieghere F, Standaert AR, Geeraerd AH, Cools I, Van Impe JF, Debevere J. 2005. Environmental factors influence the relation between optical density and cell count for *Listeria monocytogenes*. J Appl Microbiol 99:1503–15.
García-Gimeno RM, Hervás-Martinez C, de Siloniz MI. 2002. Improving artificial neural networks with a pruning methodology and genetic algorithms for their application in microbial growth prediction in food. Int J Food Microbiol 72:19–30.
García-Gimeno RM, Hervás-Martinez C, Barco-Alcalá E, Zurera-Cosano G, Sanz-Tapia E. 2003. An artificial neural network approach for *Escherichia coli* O157: H7 growth estimation. J Food Sci 68:639–45.
García-Gimeno RM, Hervás-Martinez C, Rodríguez-Pérez R, Zurera-Cosano G. 2005. Modelling the growth of *Leuconostoc mesenteroides* by artificial neural networks. Int J Food Microbiol 105:317–32.
Geeraerd AH, Van Impe JF. 1999. Recent developments in describing the combined effect of temperature, pH, sodium chloride and sodium nitrite concentration on the growth of microorganisms. In: Third European Symposium on Sous Vide Proceedings 71–98. Leuven, Belgium: Katholieke Universiteit.
Geeraerd AM, Herremans CH, Cenens C, Van Impe JF. 1998. Application of artificial neural networks as a non-linear modular modelling technique to describe bacterial growth in chilled food products. Int J Food Microbiol 44:49–68.
Geeraerd AH, Valdramidis VP, Devlieghere F, Bernaert H, Debevere J, Van Impe JF. 2004. Development of a novel approach for secondary modelling in predictive microbiology: incorporation of microbiological knowledge in black box polynomial modelling. Int J Food Microbiol 91:229–44.
George SM, Richardson LCC, Peck MW. 1996. Predictive models of the effect of temperature, pH and acetic and lactic acids on the growth of *Listeria monocytogenes*. Int J Food Microbiol 32:73–90.
Giannuzzi L, Zaritzky NE. 1996. Effect of ascorbic acid in comparison to citric and lactic acid on *Listeria monocytogenes*. Inhibition at refrigeration temperatures. Lebensm-Wiss U-Technol 29:278–85.
Hajmeer M, Basheer I., Najjar Y. 1997. Computational neural networks for predictive microbiology: II. Application to microbial growth. Int J Food Microbiol 34:51–66.

Hervás C, Algar JA, Silva M. 2000. Correction for temperature variation in kinetic-based determinations with pruning computational neural networks by using genetic algorithms. J Chem Inf Comput Sci 40:724–31.
Hervás C, Zurera G, García RM, Martinez J. 2001. Optimization of computational neural network for its application to the prediction of microbial growth in foods. Food Sci Technol Int 7:159–63.
Hervás-Martínez C, García-Gimeno RM, Martinez-Estudillo AC, Martinez-Estudillo FJ, Zurera-Cosano G. 2006. Improving microbial growth prediction by product unit neural networks. J Food Sci 71(2):31–8.
Jacxsens L, Devlieghere F, Ragaert P, Vanneste E, Debevere J. 2003. Relation between microbiological quality, metabolite production and sensory quality of equilibrium modified atmosphere packaged fresh-cut produce. Int J Food Microbiol 83:263–80.
Jeyamkondan S, Jayas DS, Holley RA. 2001. Microbial growth modelling with artificial neural networks. Int J Food Microbiol 64:343–54.
Le Marc Y, Huchet V, Bourgeois CM, Guyonnet JP, Mafart P, Thuault D. 2002. Modelling the growth kinetics of *Listeria* as a function of temperature, pH and organic acid concentration. Int J Food Microbiol 73:219–37.
Lebert I., Robles-Olvera V, Lebert A. 2000. Application of polynomial models to predict growth of mixed cultures of *Pseudomonas* spp. and *Listeria* in meat. Int J Food Microbiol 61:27–39.
Lou W, Nakai S. 2001. Artificial neural network based predictive model for bacterial growth in a simulated medium of modified-atmosphere-packed cooked meat products. J Agr Food Chem 49:1799–804.
Mackey BM, Seymour DA. 1989. The bactericidal effect of isoascorbic acid combined with mild heat. J Appl Bacteriol 67:629–38.
McClure PJ, Beaumont AL, Sutherland JP, Roberts TA. 1997. Predictive modelling of growth of *Listeria monocytogenes*. The effects on growth of NaCl, pH, storage temperature and $NaNO_2$. Int J Food Microbiol 34:221–32.
Membré JM, Ross T, McMeekin T. 1999. Behaviour of *Listeria monocytogenes* under combined chilling processes. Lett Appl Microbiol 28:26–30.
Neumeyer K, Ross T, Thomson G, McMeekin TA. 1997. Validation of a model describing the effects of temperature and water activity on the growth of psychrotrophic pseudomonads. Int J Food Microbiol 38:55–63.
Nyati, H. 2000. Survival characteristics and the applicability of predictive mathematical modelling to *Listeria monocytogenes* growth in sous vide products. Int J Food Microbiol 56:123–32.
Ratkowsky DA, Olley J, McMeekin TA, Ball A. 1982. Relationship between temperature and growth rate of bacterial cultures. J Bacteriol 149:1–5.
Ross T. 1996. Indices for performance evaluation of predictive models in food microbiology. J Appl Bacteriol 81:501–8.
Ross T. 1999. Predictive microbiology for the meat industry. North Sydney. Meat and Livestock Australia.
Ross T, Dalgaard P, Tienungoon S. 2000. Predictive modelling of the growth and survival of Listeria in fishery products. Int J Food Microbiol 62:231–45.
Whiting RC, Buchanan RL. 1993. A classification of models in predictive microbiology. Food Microbiol 10:175–7.
Wijtzes T, Rombouts FM, Kant-Muermans MLT, Van`t Riet K, Zwietering MH. 1993. Development and validation of combined temperature, water activity, pH model for bacterial growth rate of *Lactobacillus curvatus*. Int J Food Microbiol 63:57–64.
Yu R, Leung P, Bienfang P. 2006. Predicting shrimp growth: artificial neural network versus nonlinear regression models. Aquacult Eng 34:26–32.
Zurera-Cosano G, Castillejo-Rodríguez AM, García-Gimeno RM, Rincón-León F. 2004. Performance of response surface vs Davey model for prediction of *Staphylococcus aureus* growth parameters under different experimental conditions. J Food Prot 67:1138–45.